8 Supplementary material

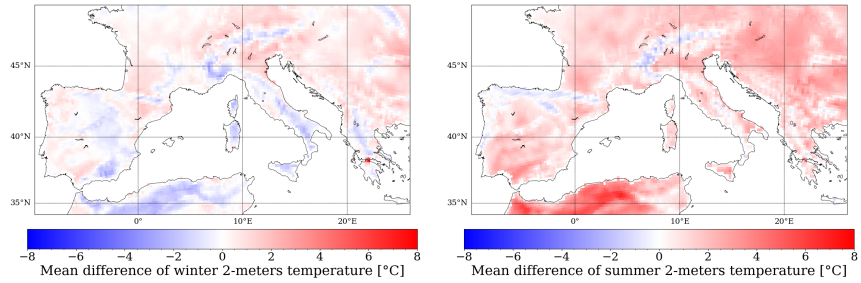

Fig. 12 Spatial distribution of the daily mean temperature difference between Med-CORDEX simulation and E-OBS observations for winter DJF (left panel) and summer JJA seasons (right panel).

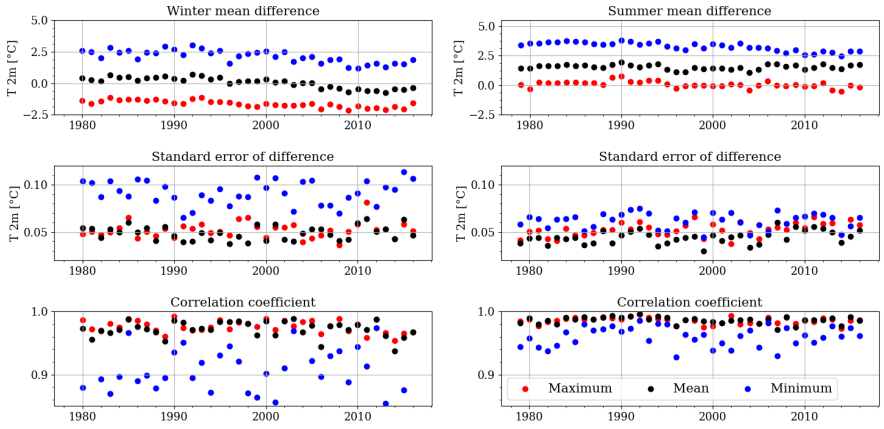

Fig. 13 Mean difference of temperature (upper row), standard error of difference (middle row), and correlation coefficient of temperature (lower row) between the Med-CORDEX simulation and E-OBS observations spatially averaged for winter, DJF, (left column) and summer, JJA, seasons (right column). Times series cover the simulation period of 1979-2016. Maximum, mean and minimum temperature are, respectively, represented by red, black, and blue color. The standard error of the difference is computed as $\sigma/\sqrt{n}$, where σ is the standard deviation of the bias and n the sample size.

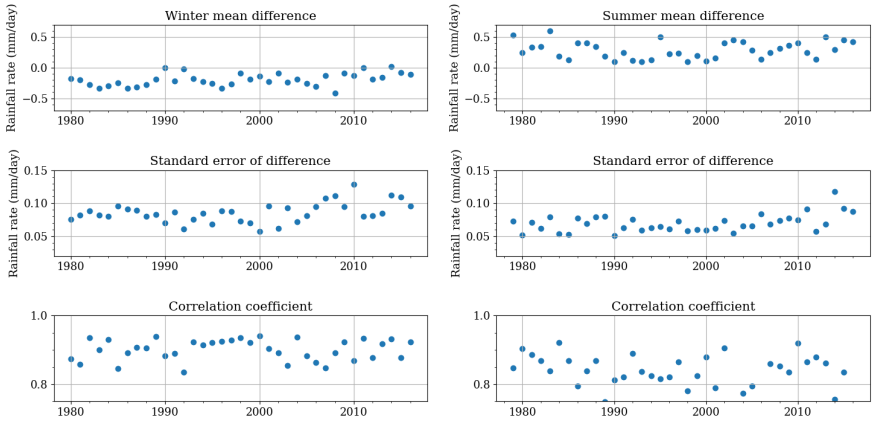

Fig. 14 Mean difference of rainfall rate (upper row), standard error of difference (middle row), and correlation coefficient of rainfall rate (lower row) between the Med-CORDEX simulation and E-OBS observations spatially averaged for winter, DJF, (left column) and summer, JJA, seasons (right column). Times series cover the simulation period of 1979-2016. The standard error of the difference is computed as $\sigma/\sqrt{n}$, where σ is the standard deviation of the bias and n the sample size.

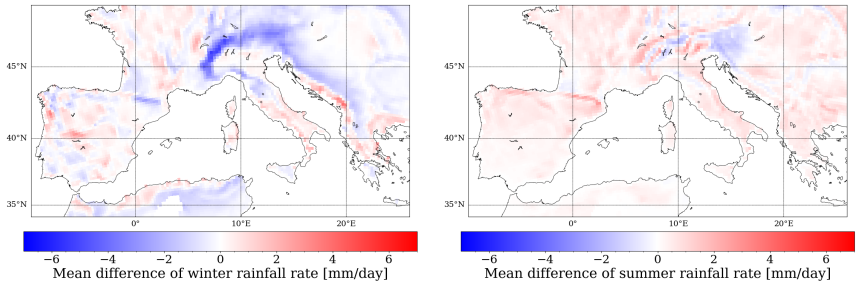

Fig. 15 Spatial distribution of the rainfall rate mean difference between the Med-CORDEX simulation and E-OBS observations for winter, DJF, (left panel) and summer, JJA, seasons (right panel).

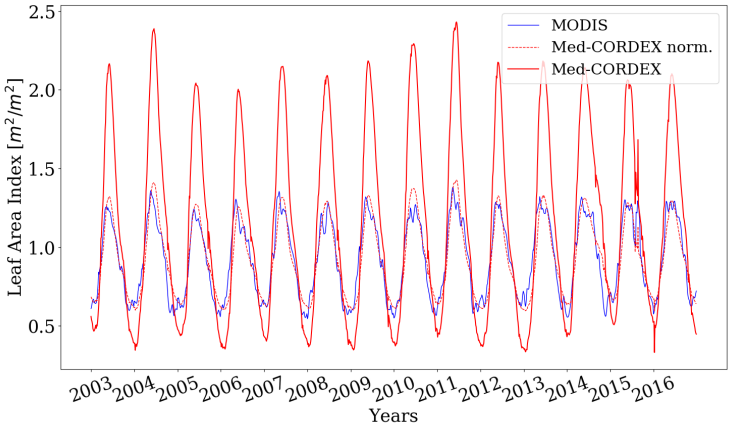

Fig. 16 Leaf Area Index simulated by the RegIPSL model (Med-CORDEX) and estimated by the MODIS satellite instrument over the 2003-2016 period. The data are spatially averaged over the Western Mediterranean. The Med-CORDEX LAI has been normalized to the regional amplitude of the MODIS LAI (red dashed line).

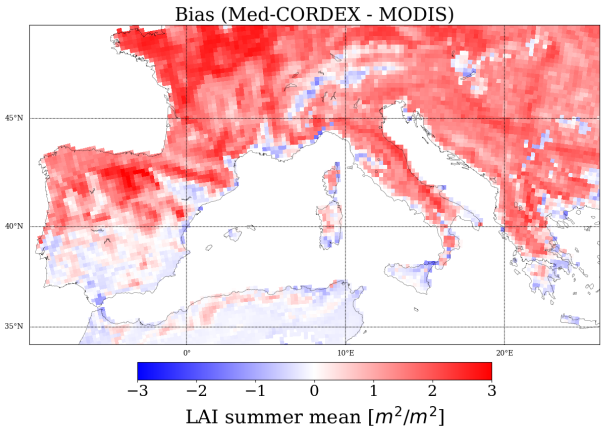

Fig. 17 Summer mean bias of the Leaf Area Index between the Med-CORDEX and MODIS over the 2003-2016 period.

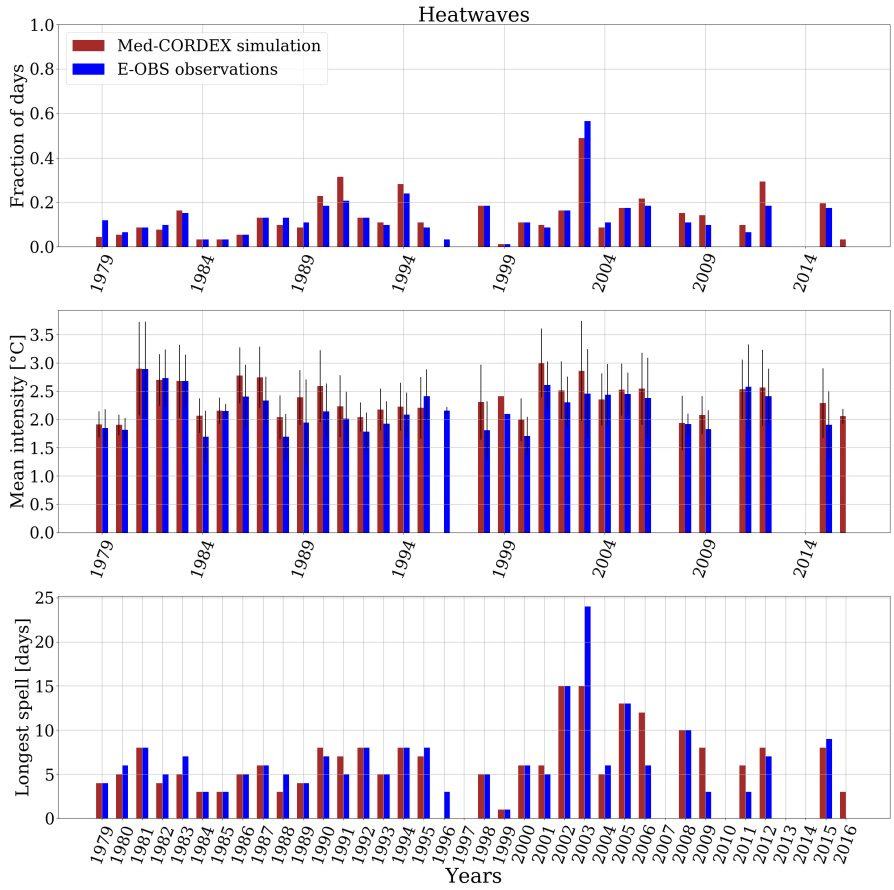

Fig. 18 Temporal variation of summer (JJA) heatwaves over the Western Mediterranean region, using the PLA_{T2m} method (on 2m temperature) from the Med-CORDEX simulation and E-OBS observations. Top panel: fraction of days affected. Middle panel: mean PLA_{T2m} (intensity). Bottom panel: duration of the longest spell in the considered season.

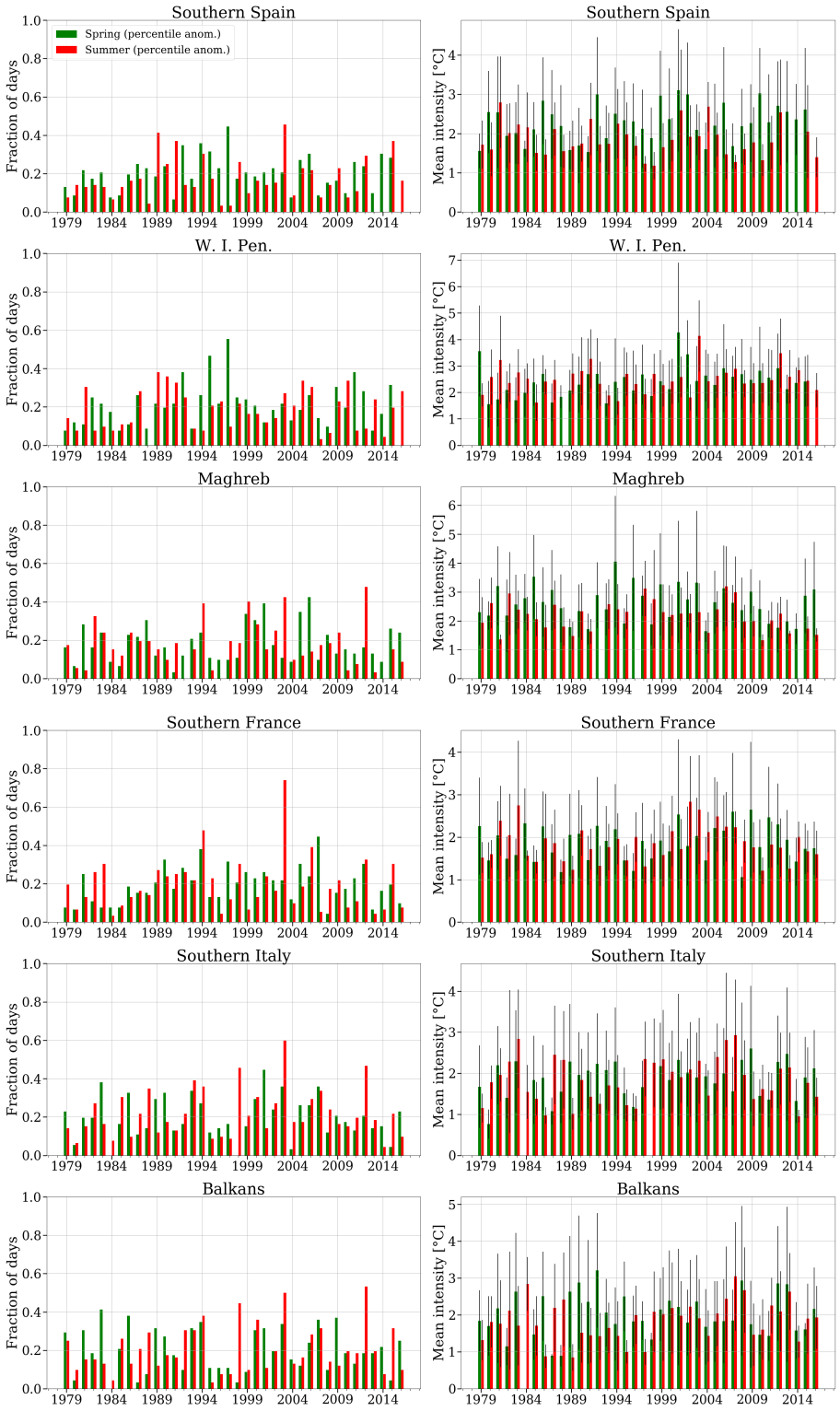

Fig. 19 Temporal variation of spring (MAM) and summer (JJA) heatwaves for the sub-regions defined in Fig. 1, using the PLA_{T2m} method (on T_{2m}). Left column: fraction of days affected. Right column: mean PLA_{T2m} and its standard deviation (error bars).

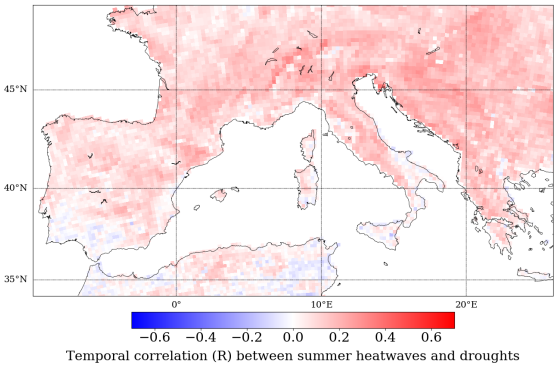

Fig. 20 Spatial distribution of the temporal correlation (R) between the summer droughts (PLA_{SD}) and heatwaves (PLA_{T2m}). A filter of significant correlation has been applied (Spearman test with p-value < 0.1).

Table 2 Mean ΔLAI in absolute and relative values between the reference cold summer (2014) and the hot summers (2003, 2009, 2011 and 2016) at the Western Mediterranean scale for the Med-CORDEX simulation (weighted sum of PFTs) and MODIS observations. ΔLAI is computed only for heatwave days. The percentage of hot days and simultaneous dry days for the considered summer is given in the fourth and fifth column. Only years with at least 10% of summer hot days are kept. The dominant PFT affected is given in the last column.

	ΔLAI obs. (m^2/m^2)	ΔLAI sim. (m^2/m^2)	Hot days (%)	Simult. dry days (%)	Dominant PFT
Balkans 2003	-0.28 (-11%)	-0.09 (-5%)	30	29	C3 agriculture
2009	0.09 (4%)	0.03 (1%)	11	3	C3 agriculture
2011	-0.05 (-1%)	-0.12 (-3%)	13	8	C3 agriculture
Maghreb 2003	-0.05 (-11%)	-0.01 (-2%)	27	4	bare soil
2009	-0.01 (-1%)	-0.01 (-1%)	16	0	bare soil
W. I. Pen. 2003	-0.10 (-7%)	-0.01 (-1%)	16	2	C3 agriculture
2009	-0.10 (-10%)	-0.11 (-9%)	11	6	C3 agriculture
2016	0.02 (2%)	-0.01 (-1%)	16	2	C3 grass
S. France 2003	-0.20 (-12%)	-0.19 (-12%)	18	8	C3 agriculture
S. Italy 2003	-0.22 (-13%)	-0.24 (-15%)	19	8	C3 grass
S. Spain 2003	-0.01 (-2%)	0.11 (14%)	36	12	C3 grass
2009	-0.02 (-3%)	0.01 (1%)	23	10	C3 grass
2011	0.07 (11%)	0.13 (17%)	38	8	C3 grass
2016	0.01 (1%)	0.03 (4%)	18	8	C3 grass
W. Medit. 2003	-0.13 (-9%)	-0.08 (-6%)	25	10	C3 grass
2009	-0.04 (-3%)	-0.04 (-3%)	12	3	C3 grass
2016	0.02 (3%)	-0.03 (-2%)	10	3	C3 grass

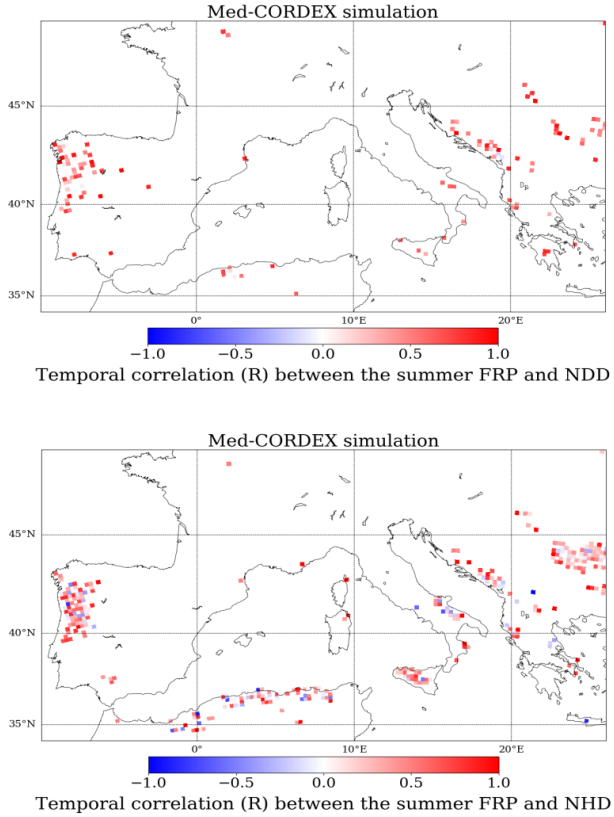

Fig. 21 Spatial distribution of temporal correlation (R) between summer Fire Radiative Power (FRP) and Number of Dry Days (top panel) for areas of high fire activity (pixels with at least 1km^2 of burned area for a minimum of 3 summers over 2003-2016). Only significant correlation (Spearman test with p-value < 0.1) are shown. The same for the correlation of the Number of Hot Days (bottom panel).